**Periodica Polytechnica Mechanical Engineering**, 68(3), pp. 234–246, 2024

# New Dimensionless Power Number Equation for Horizontal Agitated Drum

Dániel Horváth[1*], Tibor Poós[1]

[1] Department of Building Services and Process Engineering, Faculty of Mechanical Engineering, Budapest University of Technology and Economics, Műegyetem rkp. 3, H-1111 Budapest, Hungary
[*] Corresponding author, e-mail: horvath.daniel@gpk.bme.hu

Received: 07 May 2024, Accepted: 04 July 2024, Published online: 18 July 2024

**Abstract**

In dryers where mechanical mixing is applied, it is necessary to know the motor power requirement in order to design the dryer correctly. The power requirement of the motor can be traced back to the no-load power requirement and the mixing power requirement. In this study, a new dimensionless power number equation has been introduced to determine the mixing power requirement of horizontal agitated drums. A simplified form of the dimensionless power equation for the investigated agitated drum and granular material was created. The equation took into account the effect of the mixing Froude number. The values of the equation's unknown parameters were determined by a nonlinear solver using laboratory measurements. A new dimensionless number was introduced which contains the mixing power requirement and was named cohesive power number. This dimensionless number determines the relationship between the mixing power requirement and the bulk cohesion by taking into account the typical size of the mixer and the rotational speed.

**Keywords**

mixing power requirement, dimensional analysis, power number, horizontal agitated drum

## 1 Introduction

The operation of mixing occurs in many industries. The agricultural, pharmaceutical, food, mining, oil and chemical industries all performing some form of mixing task. In addition, mixing is a main or secondary task in many household appliances. In contrast to the mixing of liquids, there is no general equation for the mixing of solid granular materials that can be used to determine the mixing power requirement of the mixing engine. Several aspects complicate the description of this phenomenon. The experts use mixing apparatuses with different mixing element designs and layouts depending on the material and the purpose of mixing. There is limited literature that has been devoted to the theoretical estimation of the mixing power requirements of granular materials. The application of theoretical estimations would greatly speed up the design process of mixing apparatuses. Describing the motion of a granular mass of many discrete elements is a challenge for engineers, which makes this task even more difficult.

Gijón-Arreortúa et al. [1] described the mixing power requirement of a horizontal helical double-ribbon impeller using empirical approach and dimensional analysis. In their study, starch and icing sugar granules were mixed at different drum loading factors and rotational speeds. Empirically, the Eq. (1) was created [1]:

$$P = 0.21 n l \rho_b \mu_b V_d L_{rib} g. \tag{1}$$

The disadvantage of their equation is that it is valid only in case of the investigated mixer design, the tested materials and the investigated ranges of the rotational speed and the drum loading factor. It is not applicable to an agitated drum with paddle mixing elements. As a continuation of the research, an equation to describe the mixing power requirement was developed using dimensional analysis [1]:

$$\frac{P}{n^3 D_{rib}^{\ 5} \rho_b} = K_P \left( \frac{n^2 D_{rib}^{\ 4} \rho_b}{F_C} \right)^{-1}. \tag{2}$$

The value of the $K_p$ constant was defined as a function of the drum loading factor [1]:

$$K_P = 0.267 l + 4.261. \tag{3}$$

The term on the left side of Eq. (2) equals the power number. The member in parentheses on the right side of the

**Cite this article as:** Horváth, D., Poós, T. "New Dimensionless Power Number Equation for Horizontal Agitated Drum", Periodica Polytechnica Mechanical Engineering, 68(3), pp. 234–246, 2024. https://doi.org/10.3311/PPme.37286

equation equals the cohesion number. The mixing Froude number was neglected to make the exponent of the $K_p$ constant and the cohesion number easy to determine. For general applicability, an additional problem is that the cohesive force was measured using a particular shear box. In case of measuring with different shear boxes, different results can be obtained, even though the same material is used.

In another study, Gijón-Arreortúa et al. [2] presented a mixing power requirement equation describing a horizontal curved-ribbon impeller. The investigated materials were starch and icing sugar. In their empirically generated equation, the variables were identical as in Eq. (1), only the constant values differed [2]:

$$P = 1.03\left(nl\rho_b\mu_b V_d L_{rib} g\right)^{0.93}. \tag{4}$$

The shape of the equation generated by the dimensional analysis was the same as Eq. (2), only the equation describing the $K_p$ value was changed [2]:

$$K_P = 1.884l + 0.324. \tag{5}$$

This equation has the same problem of general applicability as in their previous study [1]. The mixing Froude number was neglected, and the cohesive force was used to create the dimensionless power number equation.

In both of Gijón-Arreortúa et al.'s works [1, 2], the exponent of the rotational speed is four in the calculation of the power number, which results in the power number having a dimension. In order for the power number to be dimensionless, the exponent of the rotational speed must be five. The axes titles on their figures already demonstrate this correctly, suggesting that the equation in the text contains typographical error. In this study, Eq. (2) demonstrates the correct form for the power number.

Wu et al. [3] have developed a theoretical equation describing the mixing power requirement in a horizontal rotary drum:

$$P = 0.086nL_d D_d^{\,3}\sin^3\alpha_l \sin\alpha_{DAoR}. \tag{6}$$

The presented equation was based on two assumptions: the particle distribution is even in each cross-section of the drum and thus the centre of bulk mass is located at the bulk geometric centre, and the granular material can be represented as a single bulk body which rotates at the same angular velocity as the drum. Therefore, this equation is also not applicable for static drums with rotating paddle mixing elements, but it provides a basis for creating the mechanical model of the apparatus.

In a previous study [4], we have created a dimensionless power number equation by using dimensional analysis to estimate the mixing power requirement in agitated drums. Based on literature, parameters affecting the mixing power requirement were collected. Based on the work of Gijón-Arreortúa et al. [1, 2], the cohesive force was considered, but the effect of the mixing Froude number was not neglected. The dimensionless power number equation of the following form was created to calculate the mixing power requirement [4]:

$$\frac{P}{L_{mp}^{\,5} n^3 \rho_b} = 43.4 l^{1.04}\left(\frac{L_{mp}^{\,4} n^2 \rho_b}{F_C}\right)^{-1}\left(\frac{L_{mp} n^2}{g}\right)^{-1/6}. \tag{7}$$

The disadvantage of this equation is based on the cohesive force. The value of the force is only valid for the direct shear box of a certain size with which it was measured.

Based on the results in the literature, the aim of this study is to create a dimensionless equation for an agitated drum that includes the bulk cohesion, instead of the cohesive force, and takes into account the effect of the mixing Froude number. The advantage of using bulk cohesion is that its value is independent of the direct shear box and depends only on the material.

## 2 Material and methods

Dimensional analysis was used to develop a dimensionless power number equation that considers both bulk cohesion and mixing Froude number. The unknown constants of the equation were determined using measurement results.

### 2.1 Material

Hulled millet (*Panicum miliaceum L.*) was used for laboratory measurements. The grains were approximated to be spherical with a characteristic size and size distribution of $d_p = 1.8 \pm 0.1$ mm [5]. The physical and material properties of the bulk at air-dry moisture content (no surface moisture) were determined in previous research [4] and are summarized in Table 1. The bulk cohesion was measured using a rectangular direct shear box [6]. The air-dry state of the bulk can be determined by the sorption isotherm of the material, which is illustrated in Fig. 1 [7].

Above the critical moisture content of $x_{crit} = 18\%$, hulled millet is no longer capable of binding additional moisture within, resulting in the appearance of moisture on the surface of the grains [7]. The surface moisture creates cohesive forces between the particles through liquid bridges. As the moisture content of the examined bulk was $x = 8.9\%$ [8] during the measurements, it was considered to be in the air-dry state.

**Table 1** Values of parameters used in dimensional analysis

| No. | Parameter name | Notation | Dimension | Value | Unit |
|---|---|---|---|---|---|
| 1 | Drum length | $L_d$ | $L$ | 0.765 | m |
| 2 | Drum width | $D_d$ | $L$ | 0.25 | m |
| 3 | Drum height | $H_d$ | $L$ | 0.27 | m |
| 4 | Mixing paddle width | $W_{mp}$ | $L$ | 0.05 | m |
| 5 | Mixing paddle height | $H_{mp}$ | $L$ | 0.02 | m |
| 6 | Mixing paddle inclination angle | $\alpha_{mp}$ | 1 | 0.1745 | rad |
| 7 | Mixing paddle force lever | $L_{mp}$ | $L$ | 0.114 | m |
| 8 | Number of mixing paddles | $N_{mp}$ | $l$ | 22 | 1 |
| 9 | Drum wall and mixing paddle surface friction coefficient | $\mu_d$ | 1 | 0.7 | rad |
| 10 | Characteristic particle size | $d_p$ | $L$ | 0.0018 ± 0.0001 | m |
| 11 | Bulk density | $\rho_b$ | $ML^{-3}$ | 867 | kgm$^3$ |
| 12 | Bulk friction coefficient | $\mu_b$ | 1 | 0.7348 | rad |
| 13 | Static angle of repose | $\alpha_{SAoR}$ | 1 | 0.6353 | rad |
| 14 | Bulk cohesion | $C_b$ | $ML^{-1}T^{-2}$ | 6568 | Pa |
| 15 | Drum loading factor | $l$ | 1 | see Table 2 | 1 |
| 16 | Rotational speed | $n$ | $T^{-1}$ | see Table 2 | s$^{-1}$ |
| 17 | Gravitational constant | $g$ | $LT^{-2}$ | 9.81 | ms$^{-2}$ |
| 18 | Mixing power requirement | $P$ | $ML^2T^{-3}$ | see Table 2 | W |

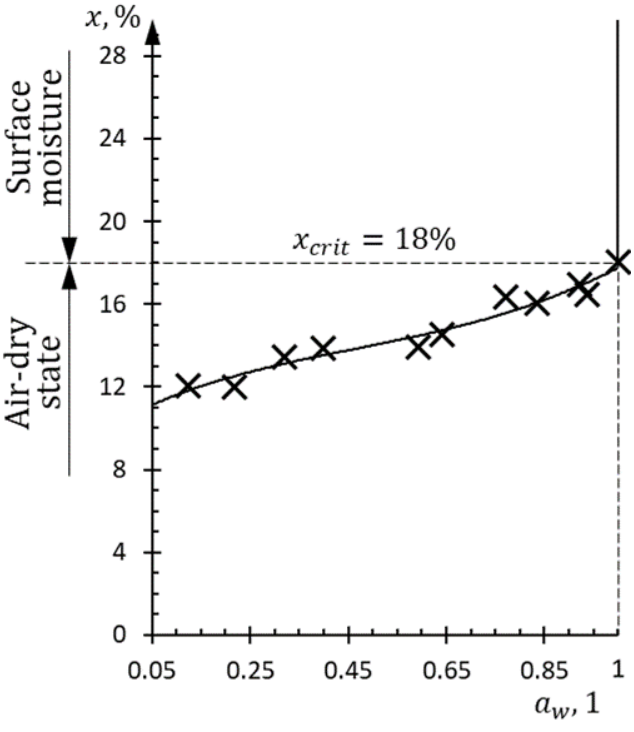


**Fig. 1** Sorption isotherm of hulled millet, based on [7]
($x$: moisture content on wet basis; $x_{crit}$: critical moisture content; $a_W$: water activity)

In case of an air-dry state bulk, we can also refer to bulk cohesion, which comprises apparent and contact cohesion [8]. Apparent cohesion is the cohesion created as a result of the shape and deformation of the grains, while contact cohesion is created by liquid bridges between the grains. Furthermore, the presence of apparent cohesion in air-dry state is also supported by the results of previous shear box measurements [6].

### 2.2 Examined horizontal agitated drum

The laboratory mixing power requirement measurements were conducted in a horizontal agitated drum dryer which is shown in Fig. 2. In order to determine the mixing power requirement at a constant material moisture content, drying was not employed in the measurements. The static drum had an U-shape and measures 765 mm in length, 250 mm in width, and 270 mm in height, resulting in an empty volume of $V_d$ = 47.4 dm$^3$. The mixing paddles, which has an inclination angle of $\alpha_{mp}$ = 10°, measures 50 mm in length, 20 mm in width, and 2 mm in thickness. The 22 *pcs* mixing paddles are attached to the Ø45 mm mixing shaft, by flat steel stems of the same cross-section turned on their edges, using removable joints. The centre lines of the blade stems are 31 mm apart. The mixing shaft is powered by a NORD SK 80 L/4 three-phase motor through a NORD SK 02-80 L/4 gearbox (gear ratio 15.95) connected by a rubber tyre coupling. The rotational speed of the mixing shaft can be adjusted using an OMRON VS mini J7 frequency converter, allowing for a range of n = 0.48 − 1.58 1/s rotational speeds. The electrical power consumption of the motor is measured by a DATCON

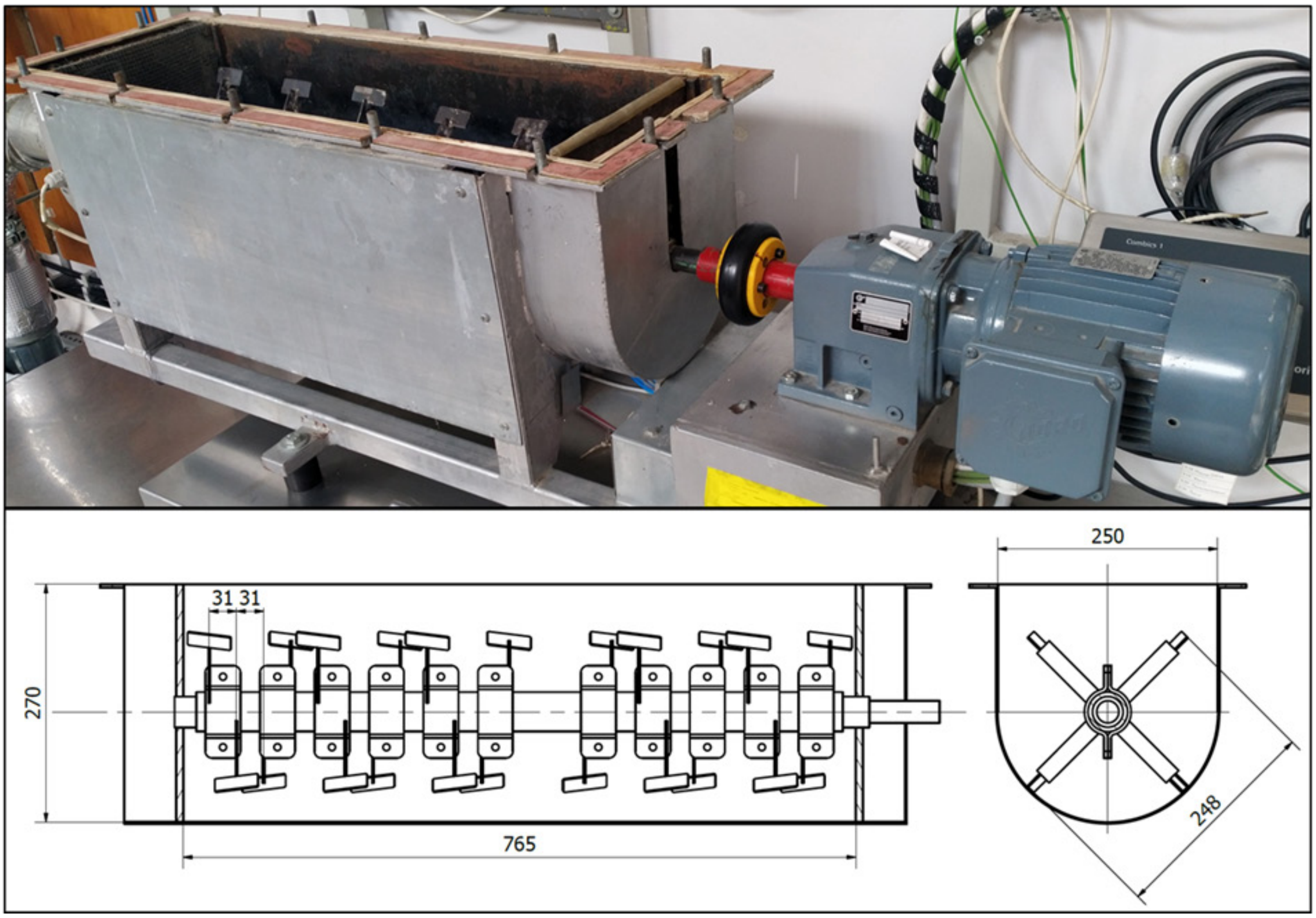


**Fig. 2** The horizontal agitated drum, and its design and main dimensions

PQRM5100 31 power transformer, which is installed between the power source and the frequency converter. The drum loading factor characterised the amount of material loaded into the drum. It is defined as the ratio of the volume of material loaded to the volume of the empty drum. Drum loading factors of $l$ = 0.1; 0.25; 0.2; and 0.25 were used in the laboratory measurements.

Previous research [8] describes the measurement method and the laboratory results. However, the values for the mixing power requirement for the $l$ = 0.25 drum loading factor were incorrectly reported. This error has been rectified in the present research.

### 2.3 Dimensional analysis

For the dimensional analysis, it is essential to collect the parameters that affect the mixing power requirement. The mixing of solid granular materials can vary, but the goal is typically to process materials quickly with a high drum loading factor and minimal operating time, which increases the mixing power requirement. When mixing granular materials, the primary operational parameters are the rotational speed [9–12], the drum loading factor for batch mixing [13, 14], and the mass or volume flow rate and hold-up for continuous mixing [3, 15]. Additionally, the no-load power requirement of the mixer [8] cannot be neglected. It results from the torque due to the design of the mixing geometry and its inertia, the friction of the components, and the air resistance. The mixing power requirement is not only influenced by the mixer geometric design [16–19] and operating parameters, but also by the material being mixed. According to [20], grains with a spherical shape require lower mixing power requirement compared to grains with an irregular shape, which require higher mixing power requirement for the same operating parameters. This is because irregularly shaped grains have higher surface friction and are more prone to entanglement. The size of the grains also determines the necessary mixing power requirement, with smaller grains requiring less and larger grains requiring more [21, 22]. This is due to the larger grains requiring more mass to be moved at once. Additionally, as the density of the grains increases, so does the mixing power requirement [23]. It is important to consider the moisture content of the materials. Moisture can alter the internal structure and size of particles in absorbent materials, affecting their properties. The sorption isotherm can identify the critical moisture content at which the material can no longer absorb moisture internally, but instead binds it to the surface, creating cohesive bonds between grains. Liquid bridges can describe the cohesive relationships. These forces hold grains together and can form agglomerates. Materials with surface moisture content require more mixing power requirement compared to those without [24].

Table 1 presents a summary of the parameters that affect the mixing power requirement, which were gathered in previous study [4] and used for dimensional analysis. The drum wall and mixing paddle surface friction coefficient was determined using discrete element method simulations in a previous study [6]. The characteristic particle size, bulk density, bulk friction coefficient, static angle of repose, and the bulk cohesion were originally determined through measurements in a previous study [8]. In this case, bulk cohesion was considered instead of the previously used cohesive force [4]. The relationship between bulk cohesion ($C_b$) and cohesive force ($F_C$) is determined by the shear cross-section ($A_{\text{shear}}$) of the applied shear box:

$$C_b = \frac{F_C}{A_{\text{shear}}}. \tag{8}$$

The value of the shear force is contingent upon the direct shear box, which may vary in size and design (e.g. shear box with circular or rectangular cross-section). By dividing the shear force by the shear cross-section, the resulting bulk cohesion becomes an independent value from the shear box. The bulk cohesion can be used more widely, since its value depends solely on the type of granular material and its moisture content.

The present study neglected two parameters: the diameter of the agitator shaft and the thickness of the agitator paddles. This was due to the low drum loading factor, resulting in minimal contact between the particles and the agitator shaft. Additionally, the paddle edges were negligibly small, resulting in negligible friction force between the paddle edges and the grains.

The dimensionless equation for the horizontal agitated drum was derived based on the parameters presented in Table 1:

$$P = f\begin{pmatrix} L_d; D_d; H_d; W_{mp}; H_{mp}; \alpha_{mp}; L_{mp}; N_{mp}; \mu_d; \\ d_p; \rho_b; \mu_b; \alpha_{SAoR}; C_b; l; n; g \end{pmatrix} \tag{9}$$

The dimensionless equation is derived using the dimensional analysis method and the basic premise known as Buckingham's ∏-theorem [25], as provided in Appendix A. The power number can be determined using the following general dimensionless equation for horizontal agitated drums:

$$\begin{aligned} N_P = &\left(\frac{l}{N_{mp}}\right)^{B_1} N_C{}^{B_2} Fr_M{}^{B_3} \left(\frac{L_d}{W_{mp}}\right)^{B_4} \left(\frac{D_d}{d_p}\right)^{B_5} \\ &\left(\frac{H_d}{H_{mp}}\right)^{B_6} \left(\frac{\alpha_{mp}}{\alpha_{SAoR}}\right)^{B_7} \left(\frac{\mu_d}{\mu_p}\right)^{B_8}. \end{aligned} \tag{10}$$

If the diameter of the mixing shaft ($D_s$) and the thickness of the mixing paddles ($S_{mp}$) had been taken into account, the right side of Eq. (10) would have been supplemented by the product of $(D_s/S_{mp})^{B9}$. In this research, the unchanged parameters were merged into a $B_0$ parameter, the value of which can therefore be considered constant. Based on these, the power number can be determined using the following simplified dimensionless equation:

$$N_P = B_0 l^{B_1} N_C{}^{B_2} Fr_M{}^{B_3}, \tag{11}$$

the power number can be expressed [26, 27]:

$$N_P = \frac{P}{L_{mp}{}^5 n^3 \rho_b}, \tag{12}$$

$B_0$ is specific to the mixer and the material, and it depends on [4]:

$$B_0 = f\left(N_{mp}; \frac{L_d}{W_{mp}}; \frac{D_d}{d_p}; \frac{H_d}{H_{mp}}; \frac{\alpha_{mp}}{\alpha_{SAoR}}; \frac{\mu_d}{\mu_b}\right), \tag{13}$$

the cohesion number that contains bulk cohesion can be expressed:

$$N_C = \frac{L_{mp}{}^2 n^2 \rho_b}{C_b}, \tag{14}$$

and the mixing Froude number can be expressed [1, 2, 4]:

$$Fr_M = \frac{L_{mp} n^2}{g}. \tag{15}$$

The value of $B_0$ was considered constant because this parameter summarises quantities that were not investigated for any changes.

When using the dimensional analysis method, there are multiple ways to obtain the final result. The equation system of the exponents in the power product requires the expression of four exponents. These exponents can be selected freely but choosing them carefully can yield additional valuable partial results. According to Appendix B, another equation was derived which takes the following form:

$$N_P = b_0 l^{b_1} N_{PC}{}^{b_2} Fr_M{}^{b_3}. \tag{16}$$

The equation introduces a new dimensionless number, $N_{PC}$, which we named the cohesive power number. This number indicates the relationship between the mixing power requirement and the bulk cohesion, while also considering the typical size of the mixer and the applied rotational speed:

$$N_{PC} = \frac{P}{C_b L_{mp}{}^3 n}. \tag{17}$$

The cohesive power number and the power number described by Eq. (12) have a close relationship, as their ratio gives the cohesion number:

$$N_C = \frac{N_{PC}}{N_P} = \frac{\dfrac{P}{C_b L_{mp}{}^3 n}}{\dfrac{P}{L_{mp}{}^5 n^3 \rho_b}} = \frac{L_{mp}{}^2 n^2 \rho_b}{C_b}. \tag{18}$$

The objective of this study is to describe the mixing power requirement. To achieve this, the unknown parameters of Eq. (11) were numerically determined using the MATLAB software *fmincon* nonlinear solver [28], as described in previous study [4]. First the values of $N_P$, $N_C$, and $Fr_M$ were calculated, and then the unknown parameters of $B_i$ ($i$ = 0, 1, 2, 3) were determined using regression analysis. According to [4], the criterion for the nonlinear solver was the least square deviation of the calculated $N_P$ values and the values predicted by Eq. (11):

$$N_{P,\min} = \min\left( \sum_{i=1}^{k} \left( \frac{N_{P,pred,i} - N_{P,calc,i}}{N_{P,calc,i}} \right)^2 \right). \tag{19}$$

The following criterion was established for the initial values of the $B_i$ parameters:

$$-2 \le B_{ini,i} \le 2, \quad B_{ini,i} \in \mathbb{Z}. \tag{20}$$

Therefore, by combining all possible integers within the examined range, a for loop examined $5^4$ = 625 initial value combinations. The final dimensionless equation was created using the combination that resulted in the smallest least square deviation. The resulting exponents were adjusted based on literature recommendations or rounded to acceptable values according to engineering considerations.

### 2.4 Statistical methods

The equation obtained from dimensional analysis was characterised by two statistical indicators. The first was the determination coefficient, which value is closer to 1, the better the fit of the function [29]:

$$R^2 = 1 - \frac{SSE}{SST} = 1 - \frac{\sum_{i=1}^{k} \left( N_{P,pred,i} - N_{P,calc,i} \right)^2}{\sum_{i=1}^{k} \left( \bar{N}_{P,calc} - N_{P,calc,i} \right)^2}. \tag{21}$$

The average relative error was another statistical indicator used to determine the fit of the function, which value is closer to 0 indicates a better fit [29]:

$$RE = \frac{100}{k} \sum_{i=1}^{k} \left( \frac{\left| N_{P,pred,i} - N_{P,calc,i} \right|}{N_{P,calc,i}} \right). \tag{22}$$

The relative errors for each power number value were also calculated [4]:

$$\delta N_P = \frac{\left| N_{P,pred} - N_{P,calc} \right|}{N_{P,calc}} 100\%. \tag{23}$$

Similar to the mean relative error, the closer the value of the relative error is to 0, the better the fit of the function at that point.

## 3 Results

In this study, a new dimensionless power number equation was created which is suitable for determining the mixing power requirement in a horizontal agitated drum. Additionally, a new dimensionless number was derived through dimensional analysis. This number describes the relationship between the mixing power requirement and the bulk cohesion, while also taking into account the typical size of the mixer and the rotational speed.

### 3.1 New dimensionless equation

Table 2 presents the mixing power requirements measured in the previous study [4] for different drum loading factors and rotational speeds. Additionally, it includes the calculated dimensionless numbers and the values of the power number predicted by the new dimensionless equation, and their relative errors.

Table 3 summarizes the constants determined using the nonlinear solver. The final exponent values were obtained in four steps, taking into account the bulk cohesion when determining the power number.

As a first step, the nonlinear solver was run without fixing the values. The results are shown in row 1 of Table 3. In the previous research [4], the exponent of the cohesion number was fixed at -1 based on Gijón-Arreortúa et al.'s work [1, 2]. However, this approach is incorrect. When expressing the power number from Eq. (18) and substituting it into Eq. (11), the cohesion number is dropped from both sides of the resulting equation. Additionally, the mixing Froude number

**Table 2** Values of the dimensionless numbers and the measured mixing power requirement [9]

| No. | $l$<br>1 | $n$<br>1/s | $P_{meas}$<br>$W$ | $N_C$<br>1 | $N_{PC}$<br>1 | $Fr_M$<br>1 | $N_{P,calc}$<br>1 | $N_{p,pred}$<br>1 | $\delta N_P$<br>% |
|---|---|---|---|---|---|---|---|---|---|
| 1 | 0.1 | 0.48 | 15.3 | 0.0004 | 3.3145 | 0.0026 | 8563 | 7442 | 13.1 |
| 2 | | 0.79 | 22.1 | 0.0011 | 2.8623 | 0.0073 | 2662 | 2298 | 13.7 |
| 3 | | 0.95 | 23.6 | 0.0015 | 2.5551 | 0.0105 | 1650 | 1511 | 8.4 |
| 4 | | 1.11 | 24.4 | 0.0021 | 2.2633 | 0.0143 | 1074 | 1060 | 1.3 |
| 5 | | 1.27 | 24.9 | 0.0028 | 2.0194 | 0.0186 | 734 | 780 | 6.3 |
| 6 | | 1.43 | 30.3 | 0.0035 | 2.1851 | 0.0236 | 627 | 595 | 5.2 |
| 7 | | 1.58 | 32.4 | 0.0043 | 2.1029 | 0.0291 | 489 | 467 | 4.5 |
| 8 | 0.15 | 0.63 | 22.4 | 0.0007 | 3.6298 | 0.0047 | 5275 | 5854 | 11.0 |
| 9 | | 0.79 | 25.6 | 0.0011 | 3.3180 | 0.0073 | 3086 | 3504 | 13.5 |
| 10 | | 0.95 | 30.3 | 0.0015 | 3.2788 | 0.0105 | 2118 | 2304 | 8.8 |
| 11 | | 1.11 | 32.5 | 0.0021 | 3.0097 | 0.0143 | 1428 | 1616 | 13.2 |
| 12 | | 1.27 | 36.7 | 0.0028 | 2.9808 | 0.0186 | 1083 | 1189 | 9.8 |
| 13 | | 1.43 | 44.2 | 0.0035 | 3.1861 | 0.0236 | 915 | 907 | 0.9 |
| 14 | | 1.58 | 44.9 | 0.0043 | 2.9149 | 0.0291 | 678 | 712 | 5.0 |
| 15 | 0.2 | 0.48 | 29.8 | 0.0004 | 6.4386 | 0.0026 | 16634 | 15302 | 8.0 |
| 16 | | 0.63 | 33.2 | 0.0007 | 5.3888 | 0.0047 | 7831 | 7896 | 0.8 |
| 17 | | 0.79 | 37.3 | 0.0011 | 4.8367 | 0.0073 | 4499 | 4726 | 5.1 |
| 18 | | 0.95 | 42.9 | 0.0015 | 4.6375 | 0.0105 | 2995 | 3107 | 3.7 |
| 19 | | 1.11 | 50.0 | 0.0021 | 4.6315 | 0.0143 | 2198 | 2180 | 0.8 |
| 20 | | 1.27 | 53.1 | 0.0028 | 4.3065 | 0.0186 | 1565 | 1603 | 2.5 |
| 21 | | 1.43 | 61.7 | 0.0035 | 4.4467 | 0.0236 | 1276 | 1223 | 4.2 |
| 22 | | 1.58 | 69.4 | 0.0043 | 4.5057 | 0.0291 | 1048 | 960 | 8.4 |
| 23 | 0.25 | 0.48 | 38.6 | 0.0004 | 8.3555 | 0.0026 | 21587 | 19299 | 10.6 |
| 24 | | 0.63 | 43.9 | 0.0007 | 7.1266 | 0.0047 | 10357 | 9958 | 3.8 |
| 25 | | 0.79 | 48.8 | 0.0011 | 6.3296 | 0.0073 | 5887 | 5961 | 1.3 |
| 26 | | 0.95 | 54.9 | 0.0015 | 5.9334 | 0.0105 | 3832 | 3919 | 2.3 |
| 27 | | 1.11 | 61.6 | 0.0021 | 5.7117 | 0.0143 | 2710 | 2749 | 1.4 |
| 28 | | 1.27 | 69.8 | 0.0028 | 5.6622 | 0.0186 | 2057 | 2022 | 1.7 |
| 29 | | 1.43 | 79.9 | 0.0035 | 5.7593 | 0.0236 | 1653 | 1542 | 6.7 |
| 30 | | 1.58 | 89.2 | 0.0043 | 5.7876 | 0.0291 | 1346 | 1210 | 10.1 |

**Table 3** The steps performed with the nonlinear solver (grey background indicates fixed values)

| Steps | $B_0$<br>1 | $B_1$<br>1 | $B_2$<br>1 | $B_3$<br>1 | max($\delta N_P$)<br>% | RE<br>% | $R^2$<br>1 |
|---|---|---|---|---|---|---|---|
| 1 | 3.15 | 1.0401 | −1.7182 | 0.5588 | 14.0 | 6.2 | 0.99 |
| 2 | 15.00 | 1.04 | −0.9013 | −0.2582 | 14.1 | 6.2 | 0.99 |
| 3 | 15.04 | 1.04 | −0.9 | −0.2594 | 14.1 | 6.2 | 0.99 |
| 4 | 15.68 | 1.04 | −0.9 | −1/4 | 13.7 | 6.2 | 0.99 |

has been neglected, resulting in a value of ${Fr_M}^{B_3}$ close to 1 and an exponent value of approximately 0. Therefore, the following equation describes the obtained inequality:

$$N_{PC} \neq B_0 l^{B_1}. \tag{24}$$

The inequality exists because $N_{PC}$ takes on several different values for a given drum loading factor, as shown in Table 2. $B_0$ and $B_1$ are constant values, so $B_3$ cannot be −1.

As a second step, the $B_1$ exponent of the drum loading factor was fixed at 1.04, as it was the same value used in previous research [4]. The solver was rerun, and the result is shown in row 2 of Table 3. The only change was a 0.1% increase in the maximum relative error.

In the third step, $B_2$ was rounded to 0.9. The solver was then rerun, and the result is shown in row 3 of Table 3. The statistical indicators' significant digits remained unchanged from the previous step.

In the fourth and final step, the exponent $B_3$ was set to 1/4 for engineering considerations. This fractional value consisting of whole numbers was the closest to the numerical value obtained in the previous step. The solver was then run again, and the result is shown in row 4 of Table 3. The maximum relative error decreased among the statistical indicators, while the values of the other indicators remained unchanged. Finally, the following dimensionless equation for the power number was obtained:

$$N_P = 15.68 l^{1.04} N_C^{-0.9} Fr_M^{-1/4}. \tag{25}$$

The final dimensionless equation for the cohesive power number was obtained by substituting the power number from Eq. (18) into Eq. (25):

$$N_{PC} = 15.68 l^{1.04} N_C^{0.1} Fr_M^{-1/4}. \tag{26}$$

Fig. 3 illustrates the measured values of the mixing power requirement and the predicted values calculated from the predicted power number as a function of the rotational speed for different drum loading factors. Fig. 3 shows that for the two lowest drum loading factors ($l$ = 0.1, 0.15), the predicted values closely approximated the measured values. However, for the two largest drum loading factors ($l$ = 0.2, 0.25), significant differences were

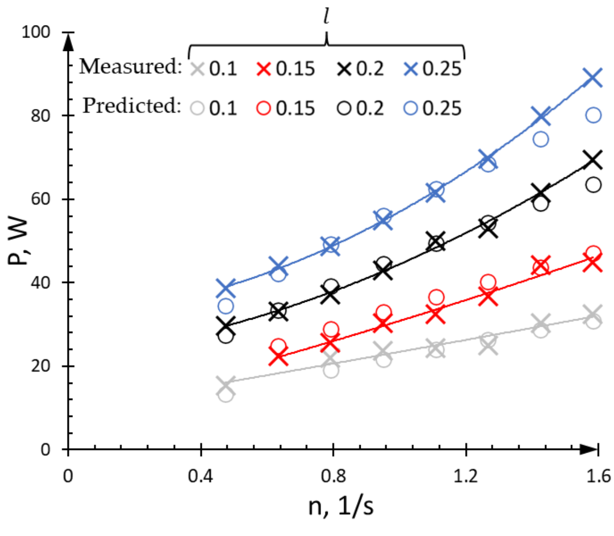


**Fig. 3** Measured and predicted mixing power requirements as a function of the rotational speed for different drum loading factors, and the trend lines fitted to the measured points in the previous study [9]

observed for $n$ = 1.43 1/$s$ and 1.58 1/s. In these cases, the dimensionless power number equation underestimated the measured values. Table 2 shows that the greatest relative error was observed at a drum loading factor of $l$ = 0.1, specifically at the rotational speed of $n$ = 0.79 1/$s$. This occurred because the measured value overestimated the trend line that was fitted in the previous research [8], while the predicted value underestimated the trend line which describes the nature of the measurement points.

Under the given conditions, Eq. (26) can be used to determine the cohesive power number of hulled millet and to calculate the mixing power requirement in the horizontal agitated drum:

- air-dry state material of x = 8.9% moisture content on wet basis,
- $10\% \leq l \leq 25\%$,
- $0.48\ 1/s \leq n \leq 1.58\ 1/s$.

The general form of the dimensionless equation given by Eq. (10) may also be applied to agitated drums of varying dimensions and geometric designs, as well as to other granular materials with spherical shapes. The implementation of bulk cohesion simplifies the use of the general dimensionless power equation for professionals in contrast to the cohesive force. In order to determine the cohesive force, it is necessary to use a specific sized shear box in each case. In contrast, the bulk cohesion can be determined with any sized shear box, as it is an equipment-independent value. In light of these considerations, the use of bulk cohesion is both expedient and justified.

### 3.2 New dimensionless cohesive power number

The cohesive power number is a dimensionless number that describes the relationship between mixing power requirement and bulk cohesion. It also considers the typical size of the mixer and the rotational speed. In the case of air-dry materials, apparent cohesion occurs in the bulk, which is created by entanglements resulting from the shape and deformations of the particles [8]. When mixing particles with surface moisture, contact cohesion always exists due to the cohesive forces of liquid bridges between particles [8]. Fig. 4 shows the evolution of the cohesive power number for different drum loading factors.

The cohesive power numbers were clearly distinguished from each other for different drum loading factors. Their characteristics could be described by a linear function with a determination coefficient of $R^2 \geq 0.94$. However, for $l$ = 0.2 and $l$ = 0.25 drum loading factors, the nature of the functions can be better represented by quadratic polynomials.

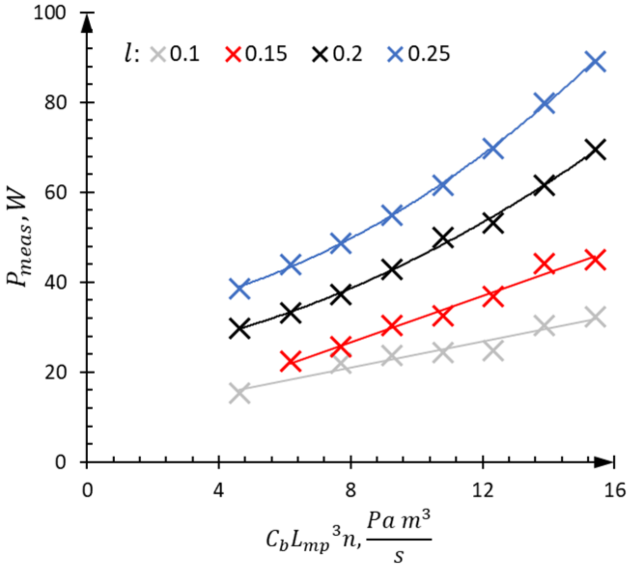


**Fig. 4** The variation of the cohesive power number in case of different drum loading factors

## 4 Conclusion

The objective of this study was to create a new dimensionless power number equation that can be used to calculate the mixing power requirement of a horizontal agitated drum when mixing granular materials. The equation was taking into account the effect of the mixing Froude number. The mixing Froude number cannot be neglected in horizontal mixers as particles tend to remain on the surface of the mixing paddles for a longer duration compared to liquids during the mixing process. Higher rotational speeds can cause particles to move with the paddles for an extended period, making the effect of gravity significant. In the new power number equation, the bulk cohesion was used instead of the cohesive force, which is a quantity independent of the direct shear box. The equation's unknown parameters were determined by using hulled millet mixing power requirement measurement results and a non-linear solver. The statistical indicators characterising the new dimensionless power number equation were the determination coefficient, the average relative error, and the maximum relative error. Based on these indicators, the new equation can predict the mixing power requirement of the horizontal agitated drum with sufficient accuracy.

A new dimensionless number, named the cohesive power number, was introduced. When mixing solid granular materials, the cohesive power number replaces the power number used for mixing liquids. This is because it considers the cohesive strength of the bulk rather than the bulk density. The cohesive power number shows the correlation between the mixing power requirement and the bulk cohesion, taking into account the typical size of the mixer and the applied rotational speed.

**Acknowledgement**

This work was supported by the János Bolyai Research Scholarship of the Hungarian Academy of Sciences (BO/00059/23/6) and by the Hungarian Scientific Research Fund (NKFIH FK-142204). The first author was supported by Gedeon Richter's Talentum Foundation (H-1103 Budapest, Gyömrői str. 19-21, Hungary). The second author was supported by the ÚNKP-23-5-BME-411 New National Excellence Program of the Ministry for Culture and Innovation from the source of the National Research, Development and Innovation Fund.

**Nomenclature**

| Latin letters | Unit | Name |
|---|---|---|
| $a_w$ | 1 | Water activity |
| $A_{shear}$ | m$^2$ | Shear cross-section of directshear box |
| $b_1, b_2, b_3, b_4$ | 1 | Equation coefficient and exponents |
| $B_1, B_2, B_3, B_4$ | 1 | Equation coefficient and exponents |
| $B_{ini,i}$ | 1 | Initial value of the equation coefficient and exponents |
| $C_b$ | Pa | Bulk cohesion |
| $d_p$ | m | Particle diameter |
| $D_d$ | m | Drum diameter |
| $D_{rib}$ | m | Ribbon mixer's outer diameter |
| $D_s$ | m | Agitator shaft diameter |
| $F_C$ | N | Cohesive force of the bulk |
| $Fr_M$ | 1 | Mixing Froude number |
| $g$ | m/s$^2$ | Gravitational constant ($g$ = 9.81 m/s$^2$) |
| $H_d$ | m | Drum height |
| $H_{mp}$ | m | Mixing paddle height |
| $i$ | 1 | Running index |
| $k$ | 1 | Maximum value of the running index |
| $K_P$ | 1 | Impeller constant |
| $l$ | 1 | Drum loading factor |
| $L_d$ | m | Drum length |
| $L_{mp}$ | m | Mixing paddle force lever |

| | | |
|---|---|---|
| $L_{rib}$ | m | Ribbon length |
| $n$ | 1/s | Rotational speed |
| $N_C$ | 1 | Cohesion number |
| $N_{mp}$ | 1 | Number of mixing paddles |
| $N_P$ | 1 | Power number |
| $N_{PC}$ | 1 | Cohesive power number |
| $N_{P,\text{calc}}$ | 1 | Calculated power number |
| $N_{P,\text{min}}$ | 1 | Power number least square deviation |
| $N_{P,\text{pred}}$ | 1 | Predicted power number |
| $P$ | W | Mixing power requirement |
| $P_{\text{meas}}$ | W | Measured mixing power requirement |
| $R^2$ | 1 | Determination coefficient |
| $RE$ | 1 | Averaged relative error |
| $S_{mp}$ | m | Mixing paddle thickness |
| $SSE$ | 1 | Sum of squared errors |
| $SST$ | 1 | Sum of squares total |
| $V_d$ | $m^3$ | Drum volume |
| $W_{mp}$ | m | Mixing paddle width |
| $x$ | % | Moisture content on wet basis |
| $x_{\text{crit}}$ | % | Critical moisture content on wet basis |
| $\mathbb{Z}$ | 1 | Set of whole numbers |
| **Greek letters** | **Unit** | **Name** |
| $\alpha_{\text{DAoR}}$ | rad | Dynamic angle of repose |
| $\alpha_l$ | rad | Drum loading degree |
| $\alpha_{mp}$ | rad | Mixing paddle inclination angle |
| $\alpha_{\text{SAoR}}$ | rad | Static angle of repose |
| $\delta N_P$ | 1 | Relative error of the power number |
| $\mu_b$ | 1 | Bulk friction coefficient |
| $\mu_d$ | rad | Drum wall and mixing paddle surface friction coefficient |
| $\rho_b$ | $kg/m^3$ | Bulk density |

## References


[1] Gijón-Arreortúa, I., Tecante, A. "Mixing Time and Power Consumption during Blending of Cohesive Food Powders with a Horizontal Helical Double-Ribbon Impeller", Journal of Food Engineering, 149, pp. 144–152, 2015. https://doi.org/10.1016/j.jfoodeng.2014.10.013

[2] Gijón-Arreortúa, I., Tecante, A. "Mixing Performance of a Curved-Ribbon Impeller during Blending of Food Powders", Chemical Engineering & Technology, 38(4), pp. 734–740, 2015. https://doi.org/10.1002/ceat.201400682

[3] Wu, W.-N., Liu, X.-Y., Zhang, R., Hu, Z. "DEM Investigation of the Power Draw for Material Movement in Rotary Drums with Axis Offset", Chemical Engineering Research and Design, 144, pp. 310–317, 2019. https://doi.org/10.1016/j.cherd.2019.02.011

[4] Horváth, D., Poós, T. "Mixing Power Requirement Determination in Agitated Drum Using Dimensional Analysis", International Journal of Engineering and Management Sciences, 8(2), pp. 76–88, 2023. https://doi.org/10.21791/IJEMS.2023.2.9

[5] Szabó, V. "Modeling of Heat and Mass Transfer in Fluidized Bed Dryers", PhD dissertation, Budapest University of Technology and Economics, 2019.

[6] Horváth, D., Tamás, K., Poós, T. "Viscoelastic Contact Model Development for the Discrete Element Simulations of Mixing Process in Agitated Drum", Powder Technology, 397, 117038, 2022. https://doi.org/10.1016/j.powtec.2021.117038

[7] Szabó, V., Poós, T., Tamás, K. "Drying Properties of Agricultural Seeds (Amaranthus l., Hordeum Vulgare, Sorghum Bicolor, Panicum Miliaceum l.)", In: EXPRES 2019: 11th International Symposium on Exploitation of Renewable Energy Sources and Efficiency, Subotica, Serbia, 2019, pp. 23–26. ISBN 978-86-919769-4-1

[8] Horváth, D., Poós, T., Tamás, K. "Modeling the Movement of Hulled Millet in Agitated Drum Dryer with Discrete Element Method", Computers and Electronics in Agriculture, 162, pp. 254–268, 2019. https://doi.org/10.1016/j.compag.2019.03.033

[9] Bao, Y., Lu, Y., Cai, Z., Gao, Z. "Effects of Rotational Speed and Fill Level on Particle Mixing in a Stirred Tank with Different Impellers", Chinese Journal of Chemical Engineering, 26(6), pp. 1383–1391, 2018. https://doi.org/10.1016/j.cjche.2017.11.010

[10] Herman, A. P., Gan, J., Zhou, Z., Yu, A. "Discrete Particle Simulation for Mixing of Granular Materials in Ribbon Mixers: A Scale-up Study", Powder Technology, 400, 117222, 2022. https://doi.org/10.1016/j.powtec.2022.117222

[11] Liu, X., Xu, X., Wu, W., Herz, F., Specht, E. "A Simplified Model to Calculate the Power Draw for Material Movement in Industrial Rotary Kilns", Powder Technology, 301, pp. 1294–1298, 2016. https://doi.org/10.1016/j.powtec.2016.08.005

[12] Li, A., Jia, F., Zhang, J., Han, Y., Meng, X., Chen, P., Wang, Y., Zhao, H. "The Effects of Filling Level on the Milling Accuracy of Rice in the Friction Rice Mill", Powder Technology, 398, 117052, 2022. https://doi.org/10.1016/j.powtec.2021.117052

[13] Cleary, P. W. "Predicting Charge Motion, Power Draw, Segregation and Wear in Ball Mills Using Discrete Element Methods", Minerals Engineering, 11(11), pp. 1061–1080, 1998. https://doi.org/10.1016/S0892-6875(98)00093-4

[14] Larsson, S., Pålsson, B. I., Parian, M., Jonsén, P. "A Novel Approach for Modelling of Physical Interactions between Slurry, Grinding Media and Mill Structure in Wet Stirred Media Mills", Minerals Engineering, 148, 106180, 2020. https://doi.org/10.3390/min11010055

[15] Sun, H., Ma, H., Zhao, Y. "DEM Investigation on Conveying of Non-Spherical Particles in a Screw Conveyor", Particuology, 65, pp. 17–31, 2022. https://doi.org/10.1016/j.partic.2021.06.009

[16] Bao, Y., Li, T., Wang, D., Cai, Z., Gao, Z. "Discrete Element Method Study of Effects of the Impeller Configuration and Operating Conditions on Particle Mixing in a Cylindrical Mixer", Particuology, 49, pp. 146–158, 2020. https://doi.org/10.1016/j.partic.2019.02.002

[17] Hu, L., Zhu, H., Hua, J. "DEM Simulation of Energy Transitions in a Hammer Mill: Effect of Impeller Configurations, Agitation Speed, and Fill Level", Powder Technology, 394, pp. 1077–1093, 2021. https://doi.org/10.1016/j.powtec.2021.08.090

[18] Zuo, Z., Gong, S., Xie, G. "Numerical Investigation of Granular Mixing in an Intensive Mixer: Effect of Process and Structural Parameters on Mixing Performance and Power Consumption", Chinese Journal of Chemical Engineering, 32, pp. 241–252, 2021. https://doi.org/10.1016/j.cjche.2020.10.036

[19] Hlosta, J., Žurovec, D., Rozbroj, J., Ramírez-Gómez, Á., Nečas, J., Zegzulka, J. "Analysis and Optimization of Material Flow inside the System of Rotary Coolers and Intake Pipeline via Discrete Element Method Modelling", Energies, 11(7), 1849, 2018. https://doi.org/10.3390/en11071849

[20] Zheng, C., Govender, N., Zhang, L., Wu, C.-Y. "GPU-Enhanced DEM Analysis of Flow Behaviour of Irregularly Shaped Particles in a Full-Scale Twin Screw Granulator", Particuology, 61, pp. 30–40, 2022. https://doi.org/10.1016/j.partic.2021.03.007

[21] Jayasundara, C. T., Yang, R. Y., Yu, A. B., Curry, D. "Discrete Particle Simulation of Particle Flow in IsaMill—Effect of Grinding Medium Properties", Chemical Engineering Journal, 135(1), pp. 103–112, 2008. https://doi.org/10.1016/j.cej.2007.04.001

[22] Tamrakar, A., Chen, S.-W., Ramachandran, R. "A DEM Model-Based Study to Quantitatively Compare the Effect of Wet and Dry Binder Addition in High-Shear Wet Granulation Processes", Chemical Engineering Research and Design, 142, pp. 307–326, 2019. https://doi.org/10.1016/j.cherd.2018.12.016

[23] Chandratilleke, G. R., Jin, X., Shen, Y. S. "DEM Study of Effects of Particle Size and Density on Mixing Behaviour in a Ribbon Mixer", Powder Technology, 392, pp. 93–107, 2021. https://doi.org/10.1016/j.powtec.2021.06.058

[24] Jin, X., Wang, S., Shen, Y. "DEM Study of Mixing Behaviours of Cohesive Particles in a U-Shaped Ribbon Mixer", Powder Technology, 399, 117097, 2022. https://doi.org/10.1016/j.powtec.2021.117097

[25] Gupta, G. S., Sarkar, S., Chychko, A., Teng, L. D., Nzotta, M., Seetharaman, S. "Chapter 3.1 - Process Concept for Scaling-Up and Plant Studies", In: Seetharaman, S. (ed.) Treatise on Process Metallurgy, Elsevier, 2014, pp. 1100–1144. https://doi.org/10.1016/B978-0-08-096988-6.00040-7

[26] Jaszczur, M., Młynarczykowska, A., Demurtas, L. "Effect of Impeller Design on Power Characteristics and Newtonian Fluids Mixing Efficiency in a Mechanically Agitated Vessel at Low Reynolds Numbers", Energies, 13(3), 640, 2020. https://doi.org/10.3390/en13030640

[27] Wang, S., Wang, P., Yuan, J., Liu, J., Si, Q., and Li, D. "Simulation Analysis of Power Consumption and Mixing Time of Pseudoplastic Non-Newtonian Fluids with a Propeller Agitator", Energies, 15(13), 4561, 2022. https://doi.org/10.3390/en15134561

[28] "Find Minimum of Constrained Nonlinear Multivariable Function - MATLAB Fmincon", [online] Available at: https://www.mathworks.com/help/optim/ug/fmincon.html [Accessed: 17 Oct 2022]

[29] Varju, E., Poós, T. "New Dimensionless Correlation for Mass Transfer at Evaporation of Open Liquid Surface in Natural Convection", International Communications in Heat and Mass Transfer, 136, 106102, 2022. https://doi.org/10.1016/j.icheatmasstransfer.2022.106102

## Appendix A

It is necessary to collect the parameters affecting the examined quantity before applying Buckingham's ∏-theorem [25]. The mixing power requirement of the horizontal agitated drum depends on 17 *pcs* considered parameters, which are summarized in Eq. (9) and Table 1.

The product of powers:

$$\prod \begin{matrix} L_d^{\alpha} D_d^{\beta} H_d^{\gamma} W_{mp}^{\delta} H_{mp}^{\varepsilon} \alpha_{mp}^{\eta} L_{mp}^{\theta} N_{mp}^{\kappa} \\ \mu_d^{\lambda} d_p^{\upsilon} \rho_b^{\xi} \mu_p^{o} \alpha_{SAoR}^{\pi} C_b^{\sigma} l^{\tau} n^{\chi} g^{\psi} P^{\omega}. \end{matrix} \tag{A1}$$

Substitution of dimensions:

$$\prod \begin{matrix} [L]^{\alpha} [L]^{\beta} [L]^{\gamma} [L]^{\delta} [L]^{\varepsilon} [1]^{\eta} [L]^{\theta} [1]^{\kappa} [1]^{\lambda} \\ [L]^{\upsilon} \left[ML^{-3}\right]^{\xi} [1]^{o} [1]^{\pi} \left[ML^{-1}T^{-2}\right]^{\sigma} \\ [1]^{\tau} \left[T^{-1}\right]^{\chi} \left[LT^{-2}\right]^{\psi} \left[ML^{2}T^{-3}\right]^{\omega}. \end{matrix} \tag{A2}$$

Sorting according to basic quantities:

$$\prod \begin{matrix} [L]^{\alpha+\beta+\gamma+\delta+\varepsilon+\theta+\upsilon-3\xi-\sigma+\psi+2\omega} [M]^{\xi+\sigma+\omega} \\ [T]^{-2\sigma-\chi-2\psi-3\omega} [1]^{\eta+\kappa+\lambda+o+\pi+\tau}. \end{matrix} \tag{A3}$$

The sum of the parameters in the exponents of the power product must be zero, so that the power is dimensionless. Based on this, the following four equations can be written:

$$\alpha+\beta+\gamma+\delta+\varepsilon+\theta+\upsilon-3\xi-\sigma+\psi+2\omega=0; \tag{A4}$$

$$\xi+\sigma+\omega=0; \tag{A5}$$

$$-2\sigma-\chi-2\psi-3\omega=0; \tag{A6}$$

$$\eta+\kappa+\lambda+o+\pi+\tau=0. \tag{A7}$$

The next step involves rearranging the equations by expressing a selected parameter for each equation. It is important to choose the appropriate characteristic size during this process, ensuring that the parameter describing the selected characteristic size is included in the relationship obtained at the end of the dimensional analysis. The $L_{mp}$ mixing paddle force lever was selected to determine the mixing power requirement, as the force acting on the paddles and the force lever produces the torque on the shaft, which can be used to calculate the required mixing power requirement by knowing the rotational speed [26]. The exponent for the $L_{mp}$ parameter is denoted by $\theta$. The remaining four equations were assigned random parameters. Therefore, the following equations can be written:

$$\theta = -\alpha - \beta - \gamma - \delta - \varepsilon - \upsilon - 2\sigma - \psi - 5\omega; \tag{A8}$$

$$\xi = -\sigma - \omega; \tag{A9}$$

$$\chi = -2\sigma - 2\psi - 3\omega; \tag{A10}$$

$$\kappa = -\eta - \lambda - o - \pi - \tau. \tag{A11}$$

By substituting the exponent equations back into Eq. (A1), the following power product is obtained:

$$\Pi \begin{array}{l} L_d^{\alpha} D_d^{\beta} H_d^{\gamma} W_{mp}^{\delta} H_{mp}^{\varepsilon} S_{mp}^{\varsigma} \alpha_{mp}^{\eta} \\ L_{mp}^{-\alpha-\beta-\gamma-\delta-\varepsilon-\nu+5\xi+3\sigma-\psi} D_d^{t} \\ N_{mp}^{-\eta-\lambda-o-\pi-\tau} \mu_d^{\lambda} d_p^{\nu} \rho_b^{-\sigma-\omega} \mu_p^{o} \\ \alpha_{SAoR}^{\pi} C_b^{\sigma} l^{\tau} n^{-2\sigma-2\psi-3\omega} g^{\psi} P^{\omega}. \end{array} \tag{A12}$$

After arranging the identical exponents into a power base, the following power product is obtained:

$$\Pi \begin{array}{l} \left(\frac{L_d}{L_{mp}}\right)^{\alpha} \left(\frac{D_d}{L_{mp}}\right)^{\beta} \left(\frac{H_d}{L_{mp}}\right)^{\gamma} \left(\frac{W_{mp}}{L_{mp}}\right)^{\delta} \left(\frac{H_{mp}}{L_{mp}}\right)^{\varepsilon} \\ \left(\frac{\alpha_{mp}}{N_{mp}}\right)^{\eta} \left(\frac{\mu_d}{N_{mp}}\right)^{\lambda} \left(\frac{d_p}{L_{mp}}\right)^{\nu} \left(\frac{\mu_p}{N_{mp}}\right)^{o} \\ \left(\frac{\alpha_{SAoR}}{N_{mp}}\right)^{\pi} \left(\frac{C_b}{L_{mp}^2 n^2 \rho_b}\right)^{\sigma} \left(\frac{l}{N_{mp}}\right)^{\tau} \\ \left(\frac{g}{L_{mp} n^2}\right)^{\psi} \left(\frac{P}{L_{mp}^5 n^3 \rho_b}\right)^{\omega}. \end{array} \tag{A13}$$

Eq. (A13) can be simplified by dividing the quotients with the same denominator, ensuring that their numerators have the same physical content. This simplifies the power product:

$$\Pi \begin{array}{l} \left(\frac{L_d}{W_{mp}}\right)^{\alpha'} \left(\frac{D_d}{d_p}\right)^{\beta'} \left(\frac{H_d}{H_{mp}}\right)^{\gamma'} \left(\frac{\alpha_{mp}}{\alpha_{SAoR}}\right)^{\eta'} \\ \left(\frac{\mu_d}{\mu_p}\right)^{\lambda'} \left(\frac{{L_{mp}}^2 n^2 \rho_b}{C_b}\right)^{\sigma'} \left(\frac{l}{N_{mp}}\right)^{\tau} \\ \left(\frac{L_{mp} n^2}{g}\right)^{\psi'} \left(\frac{P}{{L_{mp}}^5 n^3 \rho_b}\right)^{\omega}. \end{array} \tag{A14}$$

In Eq. (A14), $\omega$ is the exponent of the power number which can be expressed using Eq. (12). The $\psi'$ is the exponent of the mixing Froude number which is described by Eq. (15) while $\sigma'$ is the exponent of the cohesion number, as given by Eq. (14). The remaining terms in the power product represent the geometric and physical properties of the mixer and the granular material, which can be assumed constant for a specific mixer-material combination. These constants can be combined into a single parameter using Eq. (13).

The power number equation is determined by Eq. (11).

**Appendix B**

The initial equations used to derive the cohesion power number are identical to Eqs. (A1)-(A7) in Appendix A. By rearranging the exponents in a different way, the following equations are obtained:

$$\theta = -\alpha - \beta - \gamma - \delta - \varepsilon - \upsilon + 5\xi + 3\sigma - \psi; \tag{B1}$$

$$\omega = -\xi - \sigma; \tag{B2}$$

$$\chi = \sigma - 2\psi + 3\xi; \tag{B3}$$

$$\kappa = -\eta - \lambda - o - \pi - \tau; \tag{B4}$$

By substituting the exponent equations back into Eq. (A1), the following power product is obtained:

$$\Pi \begin{array}{l} {L_d}^{\alpha} {D_d}^{\beta} {H_d}^{\gamma} {W_{mp}}^{\delta} {H_{mp}}^{\varepsilon} {\alpha_{mp}}^{\eta} \\ L_{mp}^{-\alpha-\beta-\gamma-\delta-\varepsilon-\upsilon+5\xi+3\sigma-\psi} {N_{mp}}^{-\eta-\lambda-o-\pi-\tau} \\ {\mu_d}^{\lambda} {d_p}^{\upsilon} {\rho_b}^{\xi} {\mu_p}^{o} {\alpha_{SAoR}}^{\pi} {C_b}^{\sigma} l^{\tau} n^{\sigma-2\psi+3\xi} g^{\psi} P^{-\xi-\sigma}. \end{array} \tag{B5}$$

After arranging the identical exponents into a power base, the following power product is obtained:

$$\Pi\begin{matrix}\left(\frac{L_d}{L_{mp}}\right)^{\alpha}\left(\frac{D_d}{L_{mp}}\right)^{\beta}\left(\frac{H_d}{L_{mp}}\right)^{\gamma}\left(\frac{W_{mp}}{L_{mp}}\right)^{\delta}\left(\frac{H_{mp}}{L_{mp}}\right)^{\varepsilon}\\ \left(\frac{\alpha_{mp}}{N_{mp}}\right)^{\eta}\left(\frac{\mu_d}{N_{mp}}\right)^{\lambda}\left(\frac{d_p}{L_{mp}}\right)^{\nu}\left(\frac{L_{mp}^5 n^3\rho_b}{P}\right)^{\xi}\\ \left(\frac{\mu_p}{N_{mp}}\right)^{o}\left(\frac{\alpha_{SAoR}}{N_{mp}}\right)^{\pi}\left(\frac{C_b L_{mp}^3 n}{P}\right)^{\sigma}\\ \left(\frac{l}{N_{mp}}\right)^{\tau}\left(\frac{g}{L_{mp}n^2}\right)^{\psi}.\end{matrix} \tag{B6}$$

Eq. (B6) can be simplified by dividing the quotients with the same denominator, ensuring that their numerators have the same physical content. This simplifies the power product:

$$\Pi\begin{matrix}\left(\frac{L_d}{W_{mp}}\right)^{\alpha'}\left(\frac{D_d}{d_p}\right)^{\beta'}\left(\frac{H_d}{H_{mp}}\right)^{\gamma'}\left(\frac{\alpha_{mp}}{\alpha_{SAoR}}\right)^{\eta'}\left(\frac{\mu_d}{\mu_p}\right)^{\lambda'}\\ \left(\frac{P}{L_{mp}{}^5 n^3\rho_b}\right)^{\xi'}\left(\frac{P}{C_b L_{mp}{}^3 n}\right)^{\sigma'}\\ \left(\frac{l}{N_{mp}}\right)^{\tau}\left(\frac{L_{mp}n^2}{g}\right)^{\psi'}.\end{matrix} \tag{B7}$$

In Eq. (B7), $\xi'$ is the exponent of the power number which can be expressed using Eq. (12). The $\psi'$ is the exponent of the mixing Froude number which is described by Eq. (15), while $\sigma'$ is the exponent of the cohesive power number, as given by Eq. (17).

In this case, the power number equation is determined by Eq. (16).